

Characteristics of Acoustic Drivers for Efficient Coupling to Thermoacoustic Machines

Samir Gh. YAHYA, Itimad D J Azzawi, Mohammed k Abbas and Ahmed AAG AL-RUBAIY

Abstract—Thermoacoustic engines and coolers are a promising emerging technology due to its environmental friendliness and the lack of mechanical moving parts. Acoustic-to-electrical (or vice versa) transduction devices are the key components allowing for the conversion between acoustic (i.e. mechanical) and electrical energies (or vice versa). Some of researchers investigated the use of acoustic drivers in their devices due to their high acoustic power and transduction efficiency. This paper focuses on the performance analysis of a few selected acoustic drivers, available commercially, in order to provide a better understanding of their efficient utilisation in the context of coupling with thermoacoustic machines (engines or refrigerators). Six different acoustic drivers were studied using analytical solutions. The selected drivers have widely varied specifications which leads to major differences (in terms of ultimate performance) when various acoustic conditions are applied to simulate the presence of different thermoacoustic networks. Such investigation could lead to better engineering practices in coupling the drivers to thermoacoustic systems and positively influence their overall efficiency. Therefore, this study is thought to be beneficial design engineers working on thermoacoustic machines.

Keywords—Acoustic drivers, thermoacoustic devices, ultimate coupling, performance.

I. INTRODUCTION

Thermoacoustic technologies are a branch of physical sciences that combine Thermodynamics, Thermofluids and Acoustics. Here, thermal power can be converted to acoustic power using the thermoacoustic effect, whereby the high temperature gradient imposed on the solid material placed in gaseous medium generates sound waves. Similarly, a reverse thermoacoustic process is possible, whereby the acoustic waves lead to heat-pumping effects resulting in creating temperature gradients on the solid material [1-5]. Therefore, there are two main types of thermoacoustic devices possible: thermoacoustic engines and refrigerators. In thermoacoustic engines the thermal power is converted to acoustic power which could be then used for electricity generation or for cooling (e.g. by coupling a thermoacoustic refrigerator). On the other hand, thermoacoustic refrigerators create a cooling effect by consuming the acoustic power provided by the thermoacoustic engine or directly by an acoustic driver [6 and 7].

Manuscript received December 10, 2018; December 20, 2018.

Samir Ghazi YAHYA, the corresponding author, is with the Department of Mechanical Engineering, University of Diyala, Diyala, Iraq; (email: SamirYahya@engineering.uodiyala.edu.iq).

The authors (Itimad D J Azzawi, Mohammed k Abbas and Ahmed AAG AL-RUBAIY) are with the University of Diyala, Diyala, Iraq.

The authors would like to acknowledge the support from Professor Artur J. Jaworski for his valuable comments and discussions regarding the present work. Professor Artur J. Jaworski is with school of computing and engineering, University of Huddersfield, Huddersfield HD1 3DH, UK.

Thermoacoustic technologies have a number of advantages over conventional power production devices. For instance, the lack of the mechanical moving parts of thermoacoustic devices leads to their high reliability and low maintenance as no lubrication of moving parts is required. Another gain is that the working gas is an inert gas (e.g. helium or air) and in cheaper applications it is possible to use air. This makes thermoacoustic devices environmentally friendly due to the absence of the harmful ozone depleting emissions.

Acoustic drivers, whether ordinary audio-loudspeakers or purpose-designed linear alternators/motors, can be considered as an essential part of thermoacoustic devices. They are used to harvest acoustic energy to further convert to electricity in thermoacoustic engines (thermoacoustic electricity generators) or supply acoustic power from an electrical input to drive thermoacoustic refrigerators. In recent years, several thermoacoustic researchers have been focusing on the use of acoustic drivers in their devices due to their high acoustic power throughput. However, there is a considerable gap in the understanding the underlying principles of the coupling between thermoacoustic devices and acoustic drivers [8-11]. Therefore, the focus of this study will be the performance analysis of few selected acoustic drivers (available from Sunpower® Inc., 2005) [12] from the viewpoint of coupling to thermoacoustic networks. This paper aims to provide the theoretical knowledge and foundation of how to couple acoustic drivers to thermoacoustic devices efficiently in terms of electrical to acoustic power conversion or vice versa.

II. ACOUSTIC DRIVER SPECIFICATIONS, PERFORMANCE AND ANALYSIS

In this study, six acoustic drivers with different specifications and power handling capacities are considered to investigate their performance when coupled to different acoustic networks (see Table 1, 2 and 3).

TABLE 1
ACOUSTIC DRIVERS' MODELS AND POWERS (AVAILABLE FROM SUNPOWER® INC., 2005) [12].

N	Driver's model	Maximum acoustic power (when operated as an acoustic driver)	Maximum electrical power (when operated as a liner alternator)
1	1S132M	220W at 60 Hz	250W at 60 Hz
2	1S175M	500W at 60 Hz	750W at 60 Hz
3	1S226M	900W at 60 Hz	1.2KW at 60Hz
4	1S241M	1.6KW at 60Hz	2.0KW at 60Hz
5	1S297M	3.8KW at 60Hz	5.0KW at 60Hz
6	1S362M	8.0KW at 60Hz	10 KW at 60Hz

TABLE 2
ACOUSTIC DRIVERS' SPECIFICATIONS – GROUP A (AVAILABLE FROM
SUNPOWER® INC., 2005) [12].

Parameter	Acoustic driver model (Group A)		
	1S132M	1S175M	1S226M
(D), inch	1.9	2.553	3.661
(R _e), Ω	2	0.5	1
(R _m), N.s/m	7	15	26
(L), mH	46	68	33
(M), kg	0.721	1.69	3.643
(Bl), N/A	47	68	54
(K), KN/m	46	56	102
(f), Hz	60	60	60
(V ₁), volts (rms)	110	208	208
(I ₁), amps (rms)	4.0	8	15
2ξ ₁ , mm	14	17	20

TABLE 3
ACOUSTIC DRIVERS' SPECIFICATIONS – GROUP B (AVAILABLE FROM
SUNPOWER® INC., 2005) [12].

Parameter	Acoustic driver model (Group B)		
	1S241M	1S297M	1S362M
(D), inch	4.250	8.794	9.7
(R _e), Ω	1	0.4	0.25
(R _m), N.s/m	35	62	100
(L), mH	26	18	23
(M), kg	4.216	9.403	16.24
(Bl), N/A	54	53	63
(K), KN/m	125	169	188
(f), Hz	60	60	60
(V ₁), volts (rms)	208	208	380
(I ₁), amps (rms)	18	30	40
2ξ ₁ , mm	24	26	35

a. Solving the Governing Equations Analytically

The governing equations (cf. Equations 1 - 8) concerning the estimation of the acoustic power produced, electrical power consumed and efficiency of an acoustic driver, were solved and discussed in previous studies [10 and 11].

$$I_{real} + iI_{imaginary} = -\frac{1}{c_1} [\Delta p_{real} + C_2 U_{real} - C_3 U_{imaginary}] - \frac{i}{c_1} [C_3 U_{real} + \Delta p_{imaginary} + C_2 U_{imaginary}] \quad (1)$$

and

$$V_{real} + iV_{imaginary} = [R_e I_{real} - \omega L I_{imaginary} - C_1 U_{real}] + i[R_e I_{imaginary} + \omega L I_{real} - C_1 U_{imaginary}] \quad (2)$$

Where

$$\Delta p_{real} = |\Delta p_1| \cos \theta_{\Delta p_1} \quad (3)$$

$$\Delta p_{imaginary} = |\Delta p_1| \sin \theta_{\Delta p_1} \quad (4)$$

$$U_{imaginary} = |U_1| \sin \theta_{U_1} \quad (5)$$

$$U_{real} = |U_1| \cos \theta_{U_1} \quad (6)$$

$$|V_1| = \sqrt{(V_{real})^2 + (V_{imaginary})^2} \quad (7)$$

$$|I_1| = \sqrt{(I_{real})^2 + (I_{imaginary})^2} \quad (8)$$

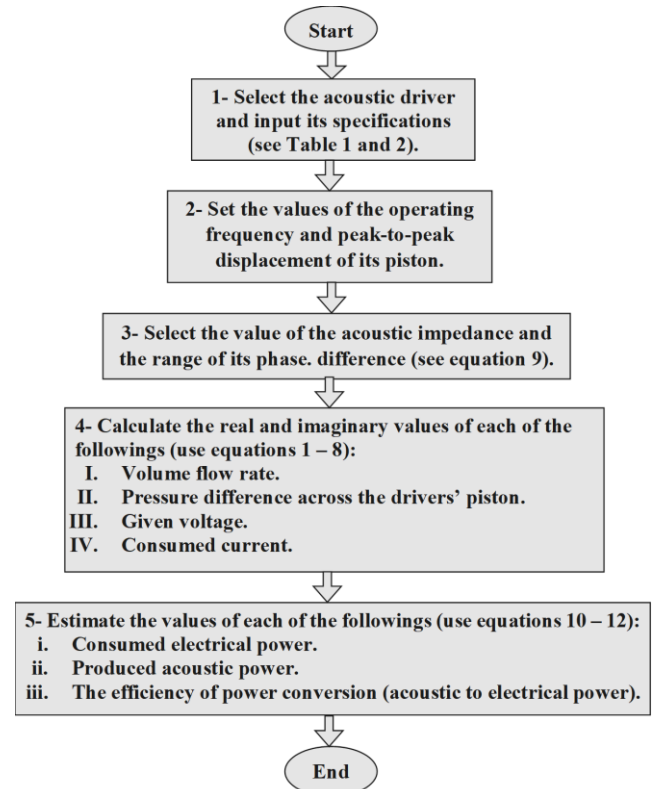
$$|Z_a| = \frac{|\Delta p_1|}{|U_1|} \quad \text{and} \quad \theta_{Z_a} = \theta_{\Delta p_1} - \theta_{U_1} \quad (9)$$

$$\dot{E}_{2,A,D} = \frac{1}{2} |\Delta p_1| |U_1| \cos \theta_{Z_a} \quad (10)$$

$$\dot{W}_e = \frac{1}{2} |I_1| |V_1| \cos \theta_{(I_1 \& V_1)} \quad (11)$$

$$\eta_{A,D} = \frac{\dot{E}_{2,A,D}}{\dot{W}_e} \quad (12)$$

In order to theoretically estimate the efficiency (understood as the value of acoustic power produced to the input electrical power, cf. Equation 12) of an acoustic driver, the complex values (real and imaginary components) of each: pressure difference $|\Delta p_1|$, volume flow rate $|U_1|$, given voltage $|V_1|$, consumed current $|I_1|$ and their relative phases should be known. Then the acoustic power produced $\dot{E}_{2,A,D}$ and the electrical power consumed \dot{W}_e by the acoustic driver can be theoretically determined (cf. Equations 10 and 11) (see flowchart 1).



Flowchart 1. Acoustic power produced, electrical power consumed and efficiency.

b. Results and Discussion

After the analytical solutions of the governing equations, the performance data of the six selected acoustic drivers (cf. Tables 1 and 2) shall be investigated and discussed. In this study, various acoustic conditions (acoustic impedance and its phase difference) are applied to achieve the highest possible efficiency of the individual acoustic drivers presented. Here, the considered range of the acoustic impedance and its phase (around acoustic driver's piston) is 10 – 50 MPa.s/m³ and - 90° to 90°, respectively when the phase of the pressure difference ($\theta_{\Delta p_1}$) is 0° while the phase of the volume flow rate (θ_{U_1}) changes from - 90° to 90° (cf. Equation (9) and Figures 1 – 6). This allows the pressure

difference to either lead or lag the volume flow rate (see Figures 1 – 6). In addition, the operating frequency (f) is set to be 60 Hz (to follow the manufacturer’s specifications) at the maximum peak-to-peak displacements of the pistons (ζ) of the acoustic drivers to achieve the highest theoretical efficiency, (cf. Tables 1 and 2).

Figure 1 illustrates the acoustic powers produced and efficiencies of the selected six acoustic drivers when connected to an acoustic network of 10 MPa.s/m³. Here, the phase of the pressure difference is either leading or lagging the volume flow rate.

This figure shows that acoustic drivers’ models (1S362M, 1S297M and 1S241M) produce the highest acoustic power among the others. However, in general their efficiencies at such acoustic impedance still considerably low. For the present considered acoustic conditions, only two out of the six acoustic drivers (models: 1S175M and 1S241M) can work with slightly higher efficiency (in terms of acoustic power produced and electrical power consumed, cf. equation 13). This means that some of the early acoustic drivers mentioned prefer higher acoustic impedance to work more efficiently (reach their highest efficiency which is around 90%). Hence, the next step was to increase the acoustic impedance from 10 to 20 MPa.s/m³ seeking higher efficiencies.

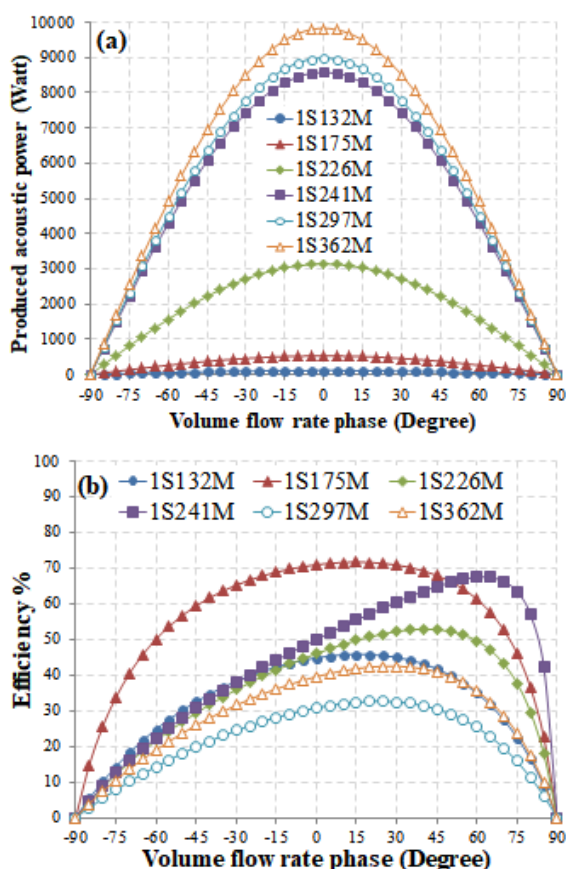


Figure 1: Acoustic drivers’ response to 10 MPa.s/m³ of acoustic impedance at different phase. (a) produced acoustic power. (b) Efficiency.

Figure 2 shows the acoustic powers produced and efficiencies of the selected six acoustic drivers when connected to an acoustic network of 20 MPa.s/m³. Here, the phase of the pressure difference is either leading or lagging the volume flow rate. It can be seen that the acoustic powers produced are considerably higher for all acoustic drivers as the acoustic impedance being increased in addition to an increase of the efficiency of acoustic drivers’ models 1S175M, 1S226M and 1S241M. On the other hand, the efficiencies of the other drivers have remarkably decreased due to the higher input electrical power required for the 20 MPa.s/m³ of acoustic impedance at all ranges of phase difference.

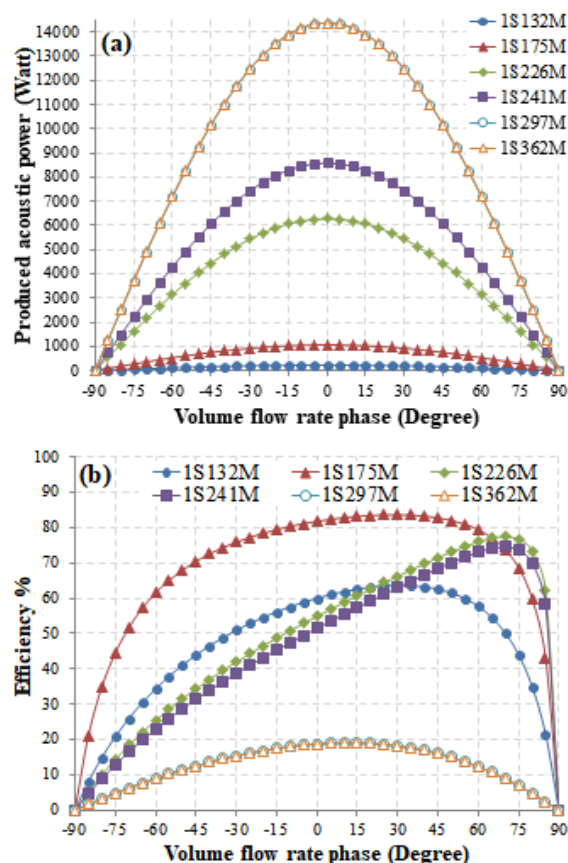


Figure 2: Acoustic drivers’ response to 20 MPa.s/m³ of acoustic impedance at different phase. (a) produced acoustic power. (b) Efficiency.

Figure 3 presents the acoustic powers produced and efficiencies of the selected six acoustic drivers when connected to an acoustic network of 30 MPa.s/m³. Here, the phase of the pressure difference is either leading or lagging the volume flow rate. In general, the acoustic power produced has slightly increased for all acoustic drivers as the acoustic impedance being increased in addition to an increase of the efficiency of acoustic driver model 1S175M to reach its maximum of almost 90%. The efficiency of the acoustic driver model 1S226M can reach 80% at only certain acoustic conditions (when the volume flow rate leading the pressure difference by 75°). However, the other drivers (model: 1S132M, 1S214M, 1S362M and 1S297M) were still showing either moderate or low efficiencies due to the unsuitable acoustic conditions.

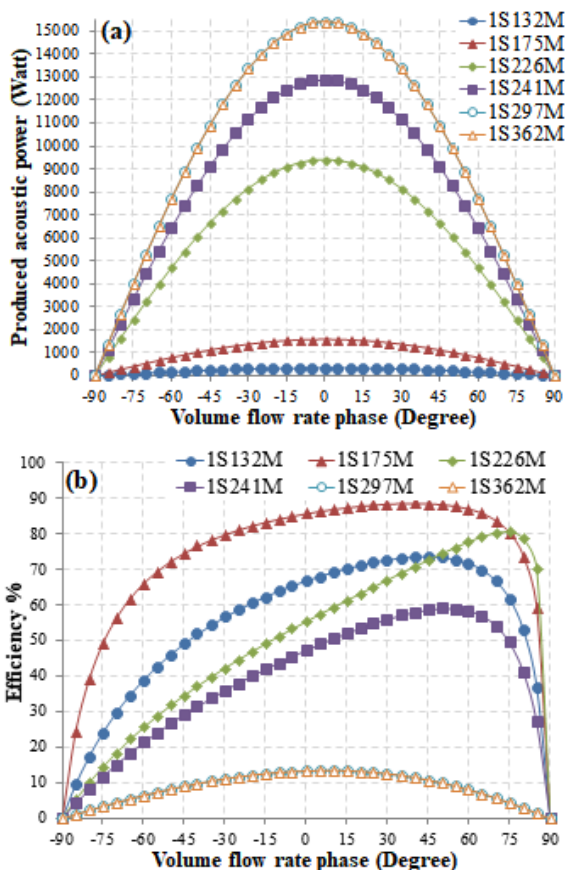


Figure 3: Acoustic drivers' response to 30 MPa.s/m³ of acoustic impedance at different phase. (a) produced acoustic power. (b) Efficiency.

Figure 4 shows the acoustic powers produced and efficiencies of the selected six acoustic drivers when connected to an acoustic network of 40 MPa.s/m³. Here, the phase of the pressure difference is either leading or lagging the volume flow rate. It can be noticed that generally the acoustic power produced has slightly increased for all acoustic drivers as the acoustic impedance being increased from 30 to 40 MPa.s/m³. This increase is also combined with an increase of the efficiencies of acoustic drivers' models 1S175M and 1S132M to reach a maximum of almost 90% and 80, respectively. Surprisingly, the efficiency of the acoustic driver model 1S226M has a slight drop to reach 70% at only certain acoustic conditions (when the volume flow rate leading the pressure difference by 60°). However, the other three drivers (model: 1S241M, 1S362M and 1S297M) were still showing either moderate or low efficiencies due to the unsuitable acoustic conditions.

Figure 5 shows the acoustic powers produced and efficiencies of the selected six acoustic drivers when connected to an acoustic network of 50 MPa.s/m³. Here, the phase of the pressure difference is either leading or lagging the volume flow rate. In general, the acoustic power produced has slightly increased for all acoustic drivers as the acoustic impedance being increased from 40 to 50 MPa.s/m³. This increase is also combined with a slight increase of the efficiencies of acoustic drivers' models 1S175M and 1S132M to exceed 90% and 80, respectively. The efficiencies of the other acoustic drivers (model: 1S362M and 1S297M) have sustained their low percentages as the acoustic impedance being increased.

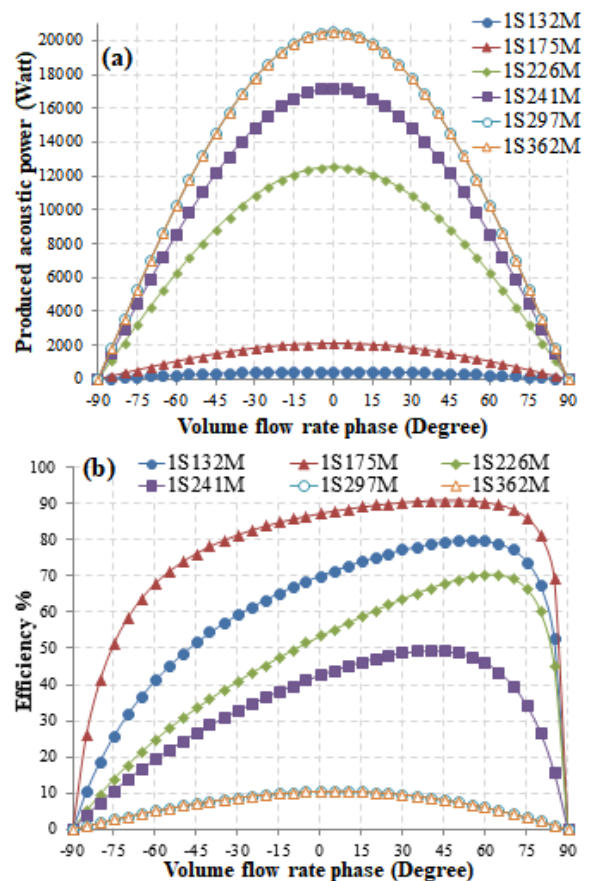


Figure 4: Acoustic drivers' response to 40 MPa.s/m³ of acoustic impedance at different phase. (a) produced acoustic power. (b) Efficiency.

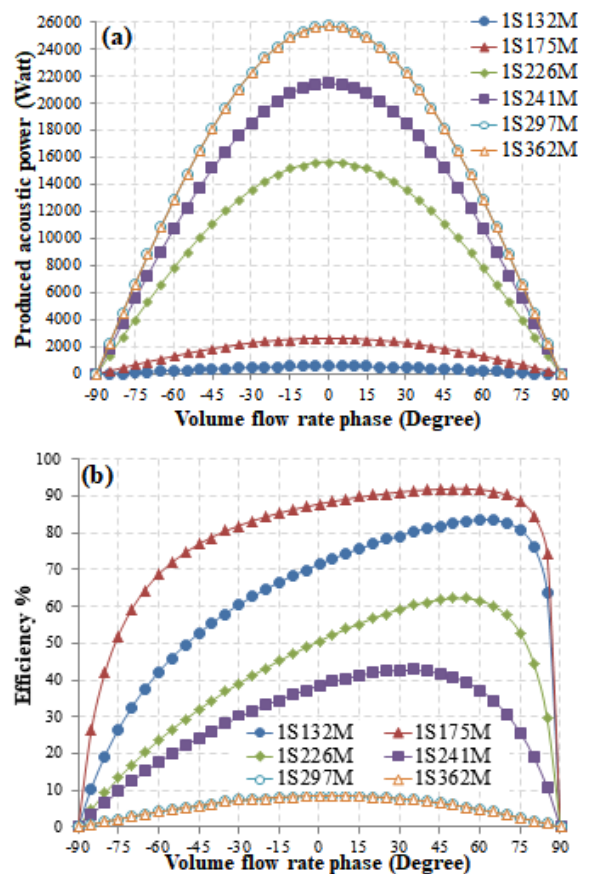


Figure 5: Acoustic drivers' response to 50 MPa.s/m³ of acoustic impedance at different phase. (a) produced acoustic power. (b) Efficiency.

It can be observed that the efficiencies of some of the selected acoustic drivers such as 1S362M and 1S297M have never reached the expected maximum values (between 80 to 90%) for the selected range of the acoustic impedance (10 to 50 MPa.s/m³). As a result, another range of the acoustic impedance was needed to improve their overall performances. Here, some of the results concerning these new sets of acoustic impedance ranges were omitted for brevity and only two values of interest (2.7 and 2.2 MPa.s/m³, see Figure 6) are presented.

Figure 6 shows the acoustic powers produced and efficiencies (theoretically achieved) of the two acoustic drivers (model: 1S362M and 1S297M) when connected to an acoustic network of 2.7 and 2.2 MPa.s/m³, respectively. Here, the phase of the pressure difference is either leading or lagging the volume flow rate. The acoustic power produced has significantly increased for both acoustic drivers as the acoustic impedance being tuned in addition to a remarkable increase of their efficiencies to exceed 85% (when the volume flow rate leading the pressure difference by 75° - 80°).

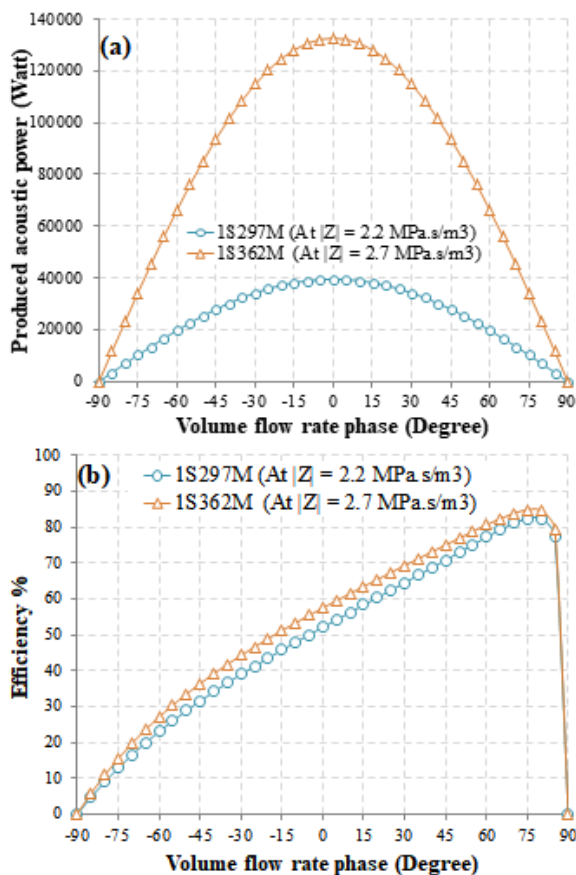


Figure 6: Acoustic drivers' (1S362M and 1S297M) response to 2.7 and 2.2 MPa.s/m³ of acoustic impedance, respectively at different phase. (a) produced acoustic power. (b) Efficiency.

III. CONCLUSION

Six different acoustic drivers (ranging from low to considerably high preferred acoustic impedance) were chosen and theoretically tested at various acoustic conditions. The current investigation provides a “map” of

operating characteristics of few selected different acoustic drivers and shows how to operate them efficiently regarding the input electrical power to the acoustic power produced by providing the suitable acoustic conditions (preferable acoustic impedance and phase difference). Such improvements in the efficiencies of the acoustic drivers' performance via an appropriate coupling to thermoacoustic networks would positively influence the overall efficiency of thermoacoustic devices. Hence, this study is thought to be beneficial for those who work in Thermoacoustics.

APPENDIX

Nomenclature

A	Cross-sectional area, m ²
\dot{E}	Acoustic power, W
f	Frequency, Hz,
I	Current, Amps
i	$\sqrt{-1}$
L	Electrical inductance of an acoustic driver, Henry
M	Moving mass, Kg
p	Pressure, Pa
R_e	Electrical resistance, Ohm
R_m	Mechanical resistance, Kg/s
U	Volumetric flow rate, m ³ /s
V	Voltage, V
\dot{W}_e	Electrical power, W
Z	Acoustic impedance, Pa.s/ m ³
Z_a	Acoustic impedance across the driver's piston
Z_e	Electrical resistance of the acoustic driver
Z_m	Mechanical impedance of the acoustic driver
Δ	Difference, Distance
ζ	Peak-to-peak displacement of driver's piston, mm
η	Efficiency, %
θ	Phase angle, degree
K	Spring constant, Nt/m
ρ	Density, kg/m ³
ω	Angular frequency, s ⁻¹
1	First order of acoustic variables, a complex amplitude
2	Second order of acoustic variables
$A.D$	Acoustic driver
$I_m[]$	Imaginary part of
$R_e[]$	Real part of
$ $	Magnitude of complex number

REFERENCES

- [1] Swift, G. W., 1988. Thermoacoustic engines. The Journal of the Acoustical Society of America 84(4), 1145-1180.
- [2] Nikolas Rott, 1980. A simple Theory of the Sondhauss Tube. Zurich.
- [3] Bisio, G. & Rubatto, G., 1999. Sondhauss and Rijke oscillations-thermodynamic analysis, possible applications and analogies. Energy, 24(2), pp.117-131.

- [4] Swift, G. (2001). Thermoacoustic: a unifying perspective for some engines and refrigerators.
- [5] Tiwatane, T., & Barve, S. (2014). Thermoacoustic Effect : the Power of Conversion of Sound Energy & Heat Energy : Review, 1(4), 20–28.
- [6] Garrett, S. L. 2004. Resource Letter: TA-1: Thermoacoustic engines and refrigerators. *American Journal of Physics*, 72, 11.
- [7] Saechan, P, Mao, X and Jaworski, AJ (2015) Optimal design of a thermoacoustic system comprising of a standing-wave engine driving a travelling-wave cooler. In: Proceedings of ICR2015. ICR2015: The 24th IIR International Congress of Refrigeration, 16-22 Aug 2015, Yokohama, Japan. International Institute of Refrigeration.
- [8] Wakeland, R. (2000). Use of electrodynamic drivers in thermoacoustic refrigerators. *The Journal of the Acoustical Society of America*, 107(2), 827–32.
- [9] Paek, I., Mongeau, L., & Braun, J. E. (2005). A method for estimating the parameters of electrodynamic drivers in thermoacoustic coolers. *The Journal of the Acoustical Society of America*, 117(1), 185. doi:10.1121/1.1828500.
- [10] Yahya S. G., Mao X. & Jaworski J. A. 2015. Design a Two-Stage Looped-tube Thermoacoustic Cooler for Thermal Management of Enclosures. The 24th IIR International Congress of Refrigeration, 16-22 Aug 2015. Yokohama, Japan: International Institute of Refrigeration.
- [11] Yahya, Samir Gh, X. Mao, and Artur J. Jaworski, "Two-stage looped-tube thermoacoustic cooler–design and preliminary testing" *Lecture Notes in Engineering and Computer Science: Proceedings of The World Congress on Engineering 2016, WCE 2016*, 29 June - 1 July, 2016, London, U.K., pp. 1044-1049.
- [12] Sunpower® Inc. (2005) Available at: <http://sunpowerinc.com/engineering-services/technology/linear-alt/> (Accessed: 30 January 2018).